GLAST LAT silicon tracker

Robert P. Johnson*
GLAST LAT Tracker Collaboration:
University of California at Santa Cruz, Japan GLAST Collaboration, INFN Bari, INFN Pisa, INFN Perugia, INFN Rome-II, INFN Trieste, Stanford Linear Accelerator Center

ABSTRACT

The Large Area Telescope (LAT) on the Gamma-ray Large-Area Space Telescope (GLAST) mission is designed to provide unprecedented sensitivity in the exploration of the gamma-ray sky. Gamma rays with energy above 10 MeV are detected via the pair conversion process, using a precision silicon tracker-converter and a hodoscopic CsI calorimeter. Charged cosmic rays are rejected by a tiled plastic-scintillator anti-coincidence detector. We report here on the design, prototyping, testing and expected performance of the silicon tracker-converter, which will be the largest silicon detector system in space after the GLAST launch in 2006. Specifically, we discuss the electronics system, the mechanical system, results from beam tests and a balloon flight, assembly procedures and prototyping experience, and expected performance of the tracker-converter.

1. INTRODUCTION

NASA's EGRET experiment on the Compton Gamma-Ray Observatory revolutionized the field of gamma-ray astronomy.[1] It was the first instrument with the effective area and background rejection necessary to detect and observe a large number of galactic and extragalactic gamma-ray sources.[2] Such sources have an inherent interest to astrophysicists and particle physicists studying high-energy, nonthermal processes, and telescopes capable of studying emission of the highest energy gamma rays play an important role in completing the broad, multi-wavelength-band coverage that is crucial to progress in modern astrophysics.

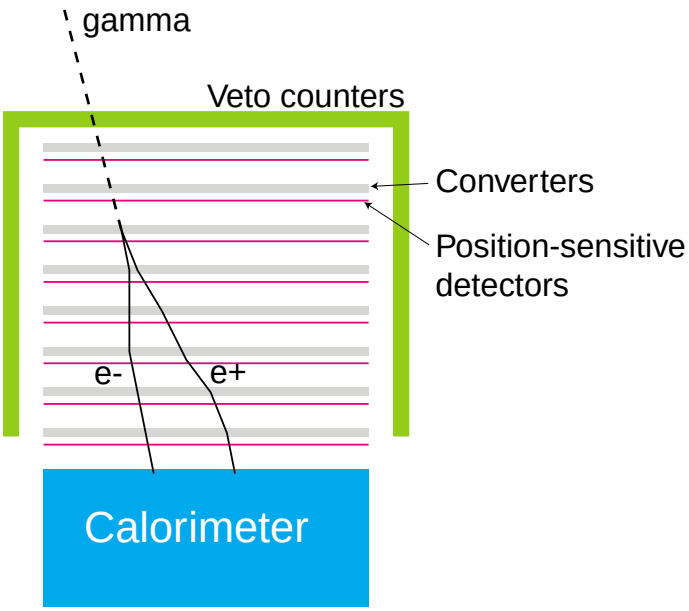

Figure 1. Pair-conversion telescope concept.

The success of EGRET and the questions raised by its discoveries demand a follow-on mission with greatly expanded capabilities. The NASA Gamma-ray Large Area Space Telescope (GLAST) mission includes two instruments: the Large Area Telescope (LAT) and a Gamma-ray Burst Monitor (GBM). The LAT is designed to improve upon the sensitivity of EGRET by a factor of 30 at 100 MeV and by even more at higher energies, including the largely unexplored 30–300 GeV band. It is being designed and built by a multinational collaboration, including scientists and engineers from France, Italy, Japan, Sweden, and the United States. The launch is scheduled for 2006, followed by an operational period of at least five years.

The LAT is a pair-conversion telescope, of the same basic concept as EGRET. Figure 1 shows a simplified sketch of such a telescope. Heavy-metal foils convert an incoming high-energy (>~10 MeV) gamma-ray into an electron-positron pair. The converters are interspersed with position-sensitive

* johnson@scipp.ucsc.edu; phone 1 831 459-2125; fax 1 831 459-5777; http://scipp.ucsc.edu/~johnson; Santa Cruz Institute for Particle Physics, University of California, Santa Cruz, CA 95064.

detectors that measure several coordinates along the electron and positron tracks. The tracks reconstructed from those coordinates are combined to give a measurement of the direction to the source of the gamma-ray, with the resolution typically limited by scattering of the particles as they pass through convert foils, detectors, and support structure. A calorimeter absorbs the electron and positron and provides a measurement of the gamma-ray energy. The veto counters surrounding the tracking part of the instrument should not fire in the case of a gamma-ray signal. However, they will register a signal from a background charged cosmic ray entering from below, through the calorimeter, as well as from above. Since charge cosmic rays (mostly protons) typically outnumber interesting gamma rays by a factor of up to 10,000, good background rejection is essential.

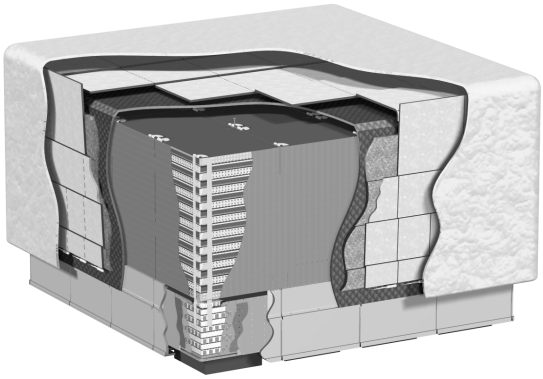

Figure 2. Cutaway view of the GLAST instrument, composed of a 4×4 array of tower modules surrounded by a veto shield and thermal blanket.

The LAT is designed to improve upon the sensitivity of EGRET by a factor of more than 30 by means of increased effective area, a much larger field-of-view, and improved angular resolution. Its layout is illustrated in Figure 2. The veto counters are greatly improved by segmentation into many tiles. This prevents loss of efficiency at high energy, as experienced by EGRET, due to firing of the veto counters by *x*-ray albedo from the electromagnetic shower in the calorimeter. In the LAT an event is vetoed only if the tracks point back to a hit tile. The calorimeter is also improved by fine segmentation. The lateral and longitudinal segmentation aids in rejection of hadronic background showers, while the longitudinal segmentation provides a means to estimate the shower leakage out the backside of the relatively thin (8.5 radiation-length) device.

The tracker/converter subsystem in the LAT achieves its excellent performance by employing silicon-strip detectors (SSDs) in place of the spark chambers that EGRET used. The newer solid-state technology offers several important advantages:

1. The LAT tracker is self-triggering. EGRET's spark chambers required an external trigger, in the form of a time-of-flight hodoscope (not shown in Figure 1), which greatly constricted its field of view.
2. The closely spaced strips of the SSDs provide excellent pattern information for background rejection and reconstruction of the conversion pair. EGRET used the time-of-flight hodoscope to eliminate background from upward-going cosmic rays, but that function can be handled in the LAT by pattern recognition algorithms. The fine strip spacing (0.228 mm) also provides good spatial resolution for reconstruction of high-energy gamma-rays (above about 1 GeV), for which multiple scattering is not necessarily the limiting factor.
3. The thin SSDs allow a near optimal arrangement of the detectors and converters for minimization of the negative impact of multiple scattering in the converter foils. The ideal is for the position-sensitive detectors to be placed immediately following the foils, to minimize the lever arm between scattering and measurement. A relatively thick gaseous detector is less suitable in this respect.
4. The SSDs can achieve close to 100% efficiency for detection of relativistic particles while maintaining very low noise. The low noise is crucial in order for the self-trigger to work and is also important for data handling and transmission. The high efficiency is crucial for good angular resolution at low energy, for if the first or second measurement following the conversion is missed, then multiple scattering seriously compromises the gamma-ray angular resolution. Just as important, if the active region of the detector is known to be 100% efficient, the reconstruction and analysis software can take advantage of that to filter out badly measured events, greatly reducing tails in the point-spread function. For example, if a track points to a 100% efficient region but does not have a hit there within the error box, then in the LAT tracker one can assume that the track was badly measured or has pattern-recognition errors.
5. The SSD readout is fast, with a dead time of only a few tens of microseconds, compared with a hundred milliseconds for spark chambers.

6. The SSDs require no consumables. EGRET's mission lifetime was limited by its supply of gas for the spark chambers.

2. TRACKER-CONVERTER DESIGN REQUIREMENTS

The design requirements revolve, first, around achieving optimal performance from the silicon-strip detector system and, second, around ensuring that the system will survive launch and operate effectively in orbit. The effective area, which determines the number of gamma-rays detected from a given flux, is a product of the geometric cross-sectional area, the conversion efficiency (determined by the converter-foil thickness), and the efficiencies for triggering, event reconstruction, and survival of all analysis selections required to eliminate background. The geometric area is limited by the rocket shroud and, ultimately, by cost. The converter-foil thickness is a compromise between effective area and angular resolution, since thicker foils cause greater multiple scattering. The number of layers of foils is limited primarily by cost of the intervening detector planes. Larger spacing of the layers enhances angular resolution at high energy but constricts the field-of-view. The detailed layout described in Section 3 makes the necessary compromises and was arrived at over a course of several years of Monte-Carlo simulation work and engineering analysis. It satisfies all of the formal science requirements set forth in the NASA Announcement of Opportunity (AO 99-055-03) for the LAT instrument of the GLAST mission.

The most important requirement for the tracker detector system is to achieve >98% efficiency in each detector plane within its fiducial area while keeping the rate of noise hits (noise occupancy) well below 1 in 10,000 channels per event trigger. This requires the combination of detector shot noise and amplifier thermal noise (plus any extraneous noise sources) to be no greater than about 2000 electrons equivalent, compared with the most probable signal from a minimum-ionizing particle at normal incidence of about 32,000 electrons (from 0.4 mm thick SSDs). For the LAT, with a total of 884,736 strips, each amplifier channel must achieve this performance while consuming no more than 210 microwatts of power (including power for digital control and readout, averaged over all channels).

It is also important for the LAT performance to minimize the non-active area between SSDs within the tracker. The tracker, like the calorimeter, is organized into 16 identical modules, as illustrated in Figure 2, partly because of limitations on the length of detector strip that can be read out with low noise but also in order to facilitate fabrication and assembly. The tracker readout electronics must fit in a minimal gap between module active areas. The SSD size itself is limited by 6-inch high-resistivity-silicon wafer technology, so small gaps also exist within each module. Much of the engineering has revolved around packaging the detectors and electronics with minimal gaps while preserving the ability to assemble each module efficiently. In fact, a tracker module can be viewed as a large, unorthodox electronics package.

The tracker support structure has to be quite substantial, compared with a high-energy-physics tracking detector, for example, because of the mass of the tungsten converter foils and the need to survive a Delta-II rocket launch. Nevertheless, it must also be highly transparent to relativistic charged particles. Conversion of a gamma ray in the support structure, rather than in a converter foil, generally leads to a poor angular measurement, especially at low energy, because the first SSD measurement will no longer be in an optimal location to minimize the effect of multiple scattering. For its low density, low Z, high strength, low coefficient of thermal expansion (CTE), and good thermal conductivity, carbon is the practically ideal material for the support structure.

The LAT tracker, with 81 square meters of silicon and nearly 900,000 readout channels, is the largest silicon-strip detector system ever designed for operation in space and is, in fact, much larger than any silicon-strip system presently operating on Earth. To ensure success in fabricating this large system with the quality control needed for space flight, the assembly must be kept simple, highly modular and repetitive, and consistent with standard techniques in the modern electronics packaging industry.

3. TRACKER-CONVERTER DESIGN CONCEPT AND LAYOUT

A single tracker module is illustrated in Figure 3. It is composed of a stack of 19 "trays," each of which is a composite panel with SSDs on top and bottom (except for the top and bottom trays, which have SSDs on one side only). The SSD strips on the top and bottom of a tray are parallel, but each tray is rotated 90° with respect to those above and below it. As a result, the strips on the bottom of one tray and those on the top of the tray below form an *x*,*y* measurement pair. Each module thus has a total of 18 such *x*,*y* pairs, each with a 2 mm vertical gap between the two planes of SSDs.

Each layer of tungsten converter foil lies immediately above an *x,y* measurement pair and is bonded to the bottom of the composite panel. A tungsten layer is made of 16 separate foils, each one matching the active area of the SSD just below it. This ensures that few gamma-ray conversions occur in the gaps between SSDs, where there would be a large scattering lever arm before reaching a measurement plane is some layer further below. The uppermost layers of tungsten are each 3% radiation-length thick. The following four layers are each 18% radiation-length thick. The lowest two *x,y* measurement pairs are not preceded by converter foils, since three *x,y* pairs is the minimum number needed to form a trigger and a good track, following a gamma-ray conversion.

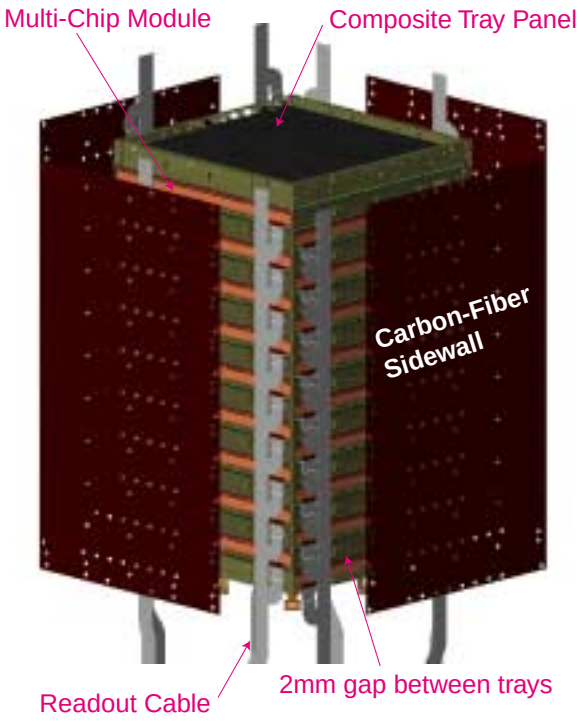

Figure 3. Exploded view of a single tracker module.

Each SSD plane is composed of 16 detectors, arranged into 4 ladders of 4 detectors each. A ladder consists of 4 detectors edge bonded, with the strips connected in series by wire bonds. Two-layer Kapton "bias circuits" are bonded to the top panel surface and to the tungsten foils on the bottom, and the SSD ladders are bonded to the bias circuits with a dot pattern of Nusil silicone-based adhesive (CV1142 and CV2646). The compliance of the adhesive is crucial to protect the silicon from thermal strain of the composite panels and, especially, the tungsten foils. Each SSD has 23 dots of adhesive, 4 of which contain conductive particles to transfer the ~100 V bias potential to the back of the detector. The top layer of the bias circuit carries this potential from the electronics module, while the bottom layer is a plane held at the reference potential of the amplifiers, to isolate the detectors and electronics from electrical fluctuations in the support structure.

The readout electronics for an SSD plane are contained on a single printed wiring board, forming a "Multi-Chip Module (MCM)." Each SSD ladder has 384 parallel strips, so an MCM must handle signals from 1536 strips. The MCM is implemented in chip-on-board technology and holds 24 front-end readout chips and two readout-controller chips, with each readout chip containing 64 amplifier-discriminator channels. The MCM is attached to one edge of the composite panel, at right angles to the SSD plane. The SSD bias and strip signals are brought around the corner by a Kapton "pitch-adapter" circuit that is bonded to a radius along the edge of the MCM, as illustrated in Figure 4. This innovative method of mounting the electronics keeps the distance from detector edge to the edge of the tracker module down to only 7 mm, thus minimizing the inactive region between tracker modules.

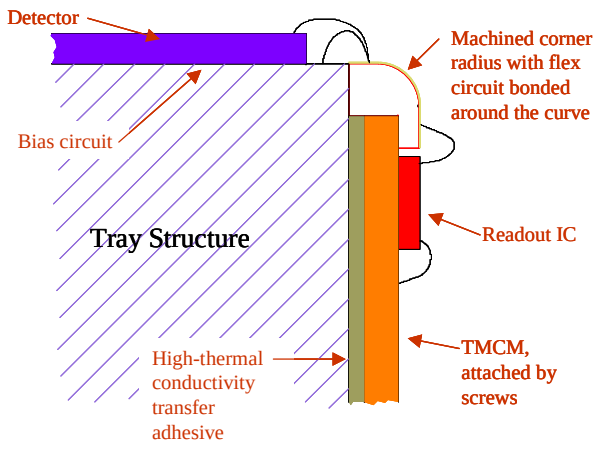

Figure 4. Integration of the readout electronics on an edge of a tray.

Two readout cables are on each of the 4 sides of a tracker module, and each cable connects to each of the 9 MCMs on the module side. The lower end of the cable extends down past the calorimeter module and connects into the Tower Electronics Module (TEM), which interfaces the tracker to the data acquisition and trigger systems. The two cables on a side form a redundant pair. They are custom 4-layer Kapton flexible circuits, which carry power, ground returns, SSD bias current, and digital communications. Each cable also holds two thermistors for temperature monitoring. They connect to the MCMs via 37-pin single-row surface-mount nano-connectors and to the TEM via 51-pin micro-D connectors. Also soldered

to the cables are SMT resistors for termination of the differential signal pairs coming from the TEM.

4. SILICON-STRIP DETECTORS

The SSDs are PIN-diodes 400 microns thick and 8.95 cm square with a high-resistivity (>5000 ohm-cm) *n*-intrinsic substrate, an aluminized *n*-type contact covering the entire backside, and *p*-type strip implants on the topside. The strip implants are 56 microns wide and spaced with a 228-micron pitch. Each strip implant has a corresponding 64-micron-wide aluminum strip above it, separated from the implant by a dielectric, which provides AC coupling to the external amplifiers. An integrated polysilicon resistor of about 50-ohms resistance biases each implant. There are 384 strips across the SSD, each with wire-bonding pads at each end. The pads are doubled to provide an extra wire-bonding area in case the first bond fails.

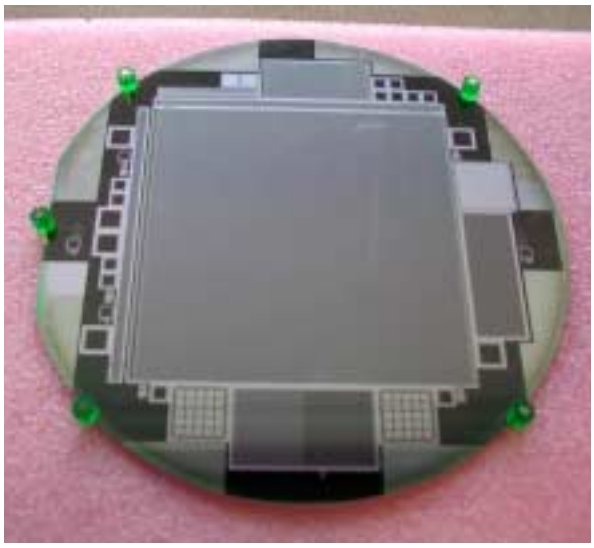

Figure 5. An SSD, before dicing from the 6-inch wafer. Numerous test structure are also visible.

A total of 10,368 SSDs are required for the 16 tracker modules plus 2 spares. More than 2000 have already been procured from Hamamatsu Photonics (HPK). They are tested at the factory against the specific LAT requirements. The quality of the delivered SSDs is remarkable, with the leakage current at room temperature less than 2.5 nA/cm^2 and with the number of bad strips less than 1 in 10,000. The very low leakage current is a major advantage for testing before and during tracker assembly, as a single bad or damaged strip can usually be detected by measurement of the total leakage current, thus avoiding time-consuming probing of the small test pads on the individual strip implants.

The SSDs are edge bonded into ladders at room temperature on a steel vacuum jig. The alignment is achieved mechanically, based on the cut edges of the SSDs. This method requires accurate dicing of the SSDs, but it allows the assembly to be fast and economical. The specified dicing tolerance is ±20 microns, but HPK has achieved a tolerance two times better than that in the delivered SSDs, with an rms deviation of only 2 microns. After edge bonding of the SSDs into a ladder, the strips are wire bonded from one SSD to the next, and the wire bonds are encapsulated by a dam-and-fill method with a silicone-based adhesive. Quality of the ladder assembly is checked by probing each aluminum strip on an automatic probe station. Measurement of the strip capacitance to the substrate can detect a broken coupling capacitor, a missing wire bond, or a short to neighboring strips.

5. READOUT ELECTRONICS

The readout electronics are based upon two custom ASICs, both implemented in the Agilent 0.5 micron CMOS process. The front-end readout chip (GTFE) has 64 two-stage charge-sensitive amplifiers, each followed by a comparator. An internal 7-bit DAC controls the common threshold of the 64 comparators. Each channel registers in the output stream only whether or not it went above threshold. The pulse height is not digitized. The chip also includes an internal calibration system, with a 7-bit DAC to set the level of the injected charge and a 64-bit register to select any subset of channels to inject charge into. Two 64-bit mask registers are located on the channel outputs, to allow any subset of channels to be disabled from the trigger output or from the data stream. A 4-event deep buffer memory stores events until the system is ready to read them out. The trigger output is simply a logical-OR of all 64 channels, while the data output is a simple shift register, with an additional feature that makes it automatically bypass if there are no hits in the event for the given chip. A control block decodes a small command set from a serial input, including register loading, calibration charge injection, and event readout.

The readout controller chip (GTRC) interfaces the GTFE chips to the TEM. Command, trigger, and clock signals from the TEM are buffered by the GTRC before going to the GTFE chips. The GTRC formats, zero suppresses, and buffers the data from the GTFE chips before sending it to the TEM. It also measures the time-over-threshold of the trigger signal, which can be useful for background rejection (to distinguish charge deposition of two electrons from that of a

single relativistic particle). Figure 6 shows a diagram of the readout system on one side of a tracker module (9 MCMs), which illustrates the redundancy designed into the system. Each GTFE chip can be controlled by either GTRC on its MCM, and each is programmed to send its data and trigger information to either the left or the right. In this way the readout can be divided into two on each MCM, with some chips shifting their data out from chip-to-chip to the left-hand GTRC and the other shifting data out to the right-hand GTRC. If a single GTFE chip on an MCM fails, all others can still be read out by reprogramming them to shift data away from the broken chip. Similarly, if a GTRC or a readout cable fails, all GTFE chips can be programmed to send their data to the opposite cable.

All essential communication is done through serial lines, with low-voltage differential signals (LVDS). Serial lines minimize the wiring and number of failure points. No output busses are used that could be brought down by a single driver failure. LVDS communication is reliable, low power, and essential for avoiding interference with the sensitive GTFE amplifiers. Great care is taken to avoid disruption of the amplifiers by digital readout activity. Note that low dead time at high rates relies upon the internal event buffering, so it is necessary that the amplifiers continue to function while previous events are being read into the GTRC chips and the TEM. We have learned that to make this works demands that the load on the power supplies from digital switching remain approximately constant throughout operation.

The self-triggering feature of the tracker is not illustrated in Figure 6 but is implemented in a simple fashion. Each GTFE chip makes a logical-OR of all of its unmasked channels and passes that information immediately and asynchronously to its neighbor, either left or right, depending on which direction it is programmed to pass data. The neighbor makes an OR of that input with its own 64-wide OR and passes the result to its neighbor, and so forth. The result is that the TEM receives a signal from each layer corresponding to logical-ORs ("layer-ORs") of all unmasked channels in that layer. Using a time window with a programmable width, the trigger electronics forms a coincidence of the layer-OR signals, normally requiring 3 consecutive *x*,*y* pairs (i.e. 6 layers) in coincidence, in order to derive a trigger. In the case of a valid trigger, a "trigger acknowledge" signal is sent back to the tracker electronics on a dedicated line about 2 microseconds (roughly the peaking time of the GTFE amplifiers) following the initial event. The GTFE chips use this signal to latch the comparator outputs into the event buffer. The price paid for this simple layer-OR trigger system is that it relies upon low noise occupancy and thus drives the noise requirements.

The MCM electronics are implemented on an 8-layer polyimide printed-wiring board (PWB) using standard surface-mount technology and chip-on-board technology, with aluminum-wire ultrasonic wedge bonding. The only non-

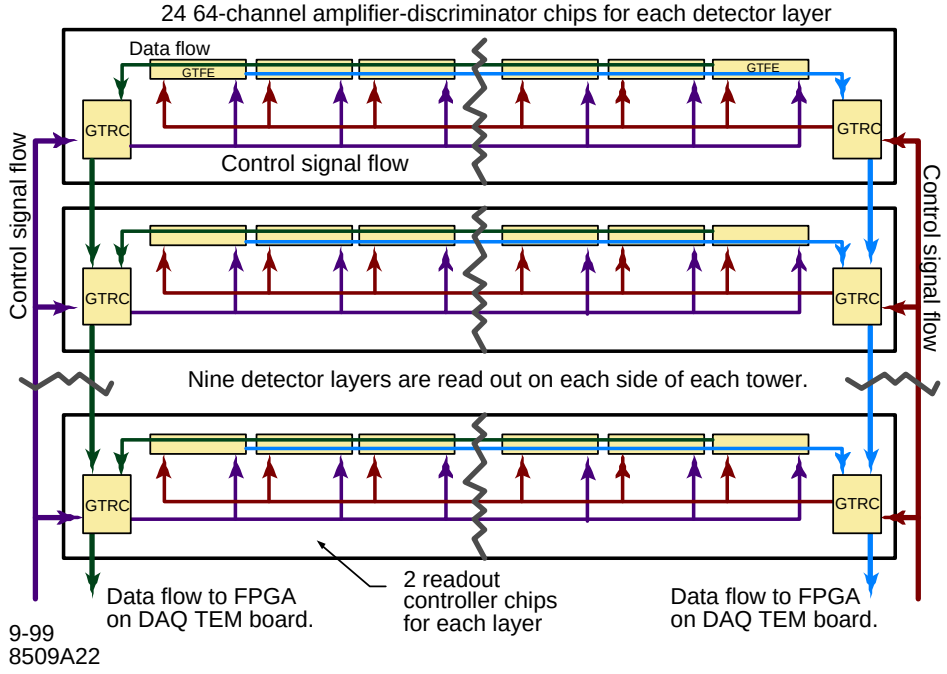

Figure 6. Simplified block diagram of the tracker readout and control system.

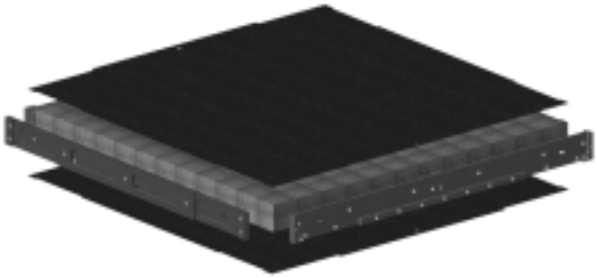

Figure 7. Exploded view of a carbon-composite tray panel (the core is aluminum honeycomb).

standard feature is the pitch-adapter flexible circuit, which has to be bonded securely around the 90° radius (see Figure 4). Special tooling has been successfully developed for this task. To produce a robust assembly for mounting onto tracker trays, the wire bonds from the ICs to the PWB and the pitch adapter are encapsulated in a hard epoxy after successful testing of the MCM. The MCMs are burned-in and thermal cycled before mounting onto trays.

The SSD ladders are the last components to be mounted onto a tray, using mechanical fixtures (no laborious optical alignment is needed). After they are bonded, wire bonds are made from the ladders to the pitch adapters of the MCM (see Figure 4). After testing, those wire bonds are encapsulated in the same way as the wire bonds between SSDs on the ladders.

We have verified that the Agilent 0.5-micron process is sufficiently radiation tolerant for our application, although radiation testing of the final chip production remains to be done. Total dose must be tested only to 10 kRad (which gives a margin of at least a factor of 5 over the expected dose on orbit). We and others[3] have verified in heavy-ion beams with prototype ICs that the threshold for single-event latchup of this epitaxial process is well above an LET of 60 MeV·cm^2/mg. Single-event-upset is only an issue in this system for the configuration registers (for example, the threshold DAC settings), so for those registers we use a radiation-hardened design.[4] We have verified with heavy ion beams that the SEU threshold is above the NASA required minimum of 8 MeV·cm^2/mg. Furthermore, analysis of the test data, together with the expected cosmic-ray flux, gives a estimate of less than one bit flip in the configuration registers of the entire tracker during 10 years of operation.

6. MECHANICAL STRUCTURE

The carbon-composite mechanical structure was engineered by a collaboration of the LAT team and Hytec Inc. of Los Alamos, NM. The structure must be sufficiently rigid that the *x* and *y* planes of SSDs do not hit each other during launch vibrations and that the tops of the 16 tracker modules do not collide. It must also conduct all of the heat generated by the tracker electronics to the tower base and into the aluminum mounting "grid" (the backbone of the LAT) with no more than an 8°C temperature drop from module top to bottom (expected leakage current in the SSDs after several years of radiation dose, and the shot noise associated with the current, limits the acceptable maximum operating temperature of the tracker). The tracker electronics cooling path travels from the MCM to the tray-panel closeout through a thermally-conductive transfer adhesive, through the closeout and into the sidewall (which is tightly clamped to a boss on the closeout by 8 screws), down the sidewall and into the closeout of the bottom tray, and from that closeout into the grid via a compressed thermal gasket. The module structure must also have good thermal stability, to minimize mechanical stress on the SSDs during temperature cycling.

Carbon is the ideal material for thermal stability, thermal conductivity, strength, and radiation transparency. The most difficult issues with regard to making a carbon-composite design are the intricate 3-D shapes needed in the closeouts of the tray panels (for mounting the MCMs, for example) and the high alignment precision required for assembly of a tracker module.

The closeout issue was resolved by machining them from carbon-carbon material with a 3-D weave of fibers. This material is the same as that used in airline brakes, but it is further heat treated and densified and finally back-filled with a small amount of resin. The result is a material that is readily machined, maintains excellent interlaminar strength, and conducts heat well through its thickness as well as laterally.

The alignment precision is achieved by assembling the 4 closeout pieces (see Figure 7) into each panel in a steel jig with room-temperature-curing adhesive. Oversized carbon-composite face sheets are first bonded to the aluminum honeycomb cores under pressure at high temperature and later trimmed to size (together with the bias circuits) after

completion of the panel assembly. Aluminum inserts are bonded into the carbon-carbon closeouts for all of the screws and alignment pins. All carbon surfaces are coated with a polymer to prevent release of dust and fibers.

The trays are supported and aligned in the tracker module by carbon-fiber composite sidewalls, as shown in Figure 3. The 1.5 mm thick sidewalls are made from a K13D graphite fiber with cyanate-ester resin. The choice of fiber and the layout of the panel plies determine the thermal conductivity of the walls, which are relied upon to carry all of the tracker electronics heat down to the module base. A 50-micron thick aluminum foil is post-bonded to the outside surface to improve the module's electrical shielding.

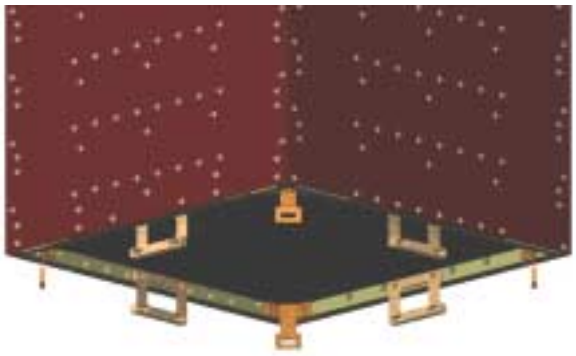

Figure 8. Flexures for mounting of a tracker module to the grid.

During assembly the trays are first aligned on two sides by dowel pins with respect to an aluminum jig, before attaching the readout cables and sidewalls to the other two sides. The sidewalls are fastened by flat-head countersunk screws. Aluminum inserts are bonded into the sidewalls for those screws that fasten the bottom tray (this joint carries by far the largest stress). The carbon-composite material holds the remaining screw heads.

There is a large thermal-expansion mismatch between the aluminum grid and the carbon-composite tracker modules. To avoid overstressing the tracker, each module is mounted to the grid via 8 flexures with titanium blades, as shown in Figure 8. The flexures also help decouple the tracker modules from deformations of the grid during vibration.

7. PROTOTYPE ASSEMBLIES AND TESTS

Several tracker prototypes have been built over the last several years and operated in beam tests, and on a balloon flight, together with prototypes of the calorimeter and veto counters. This section briefly describes those prototypes and some of the results obtained from them.

7.1 Beam test in 1997

A small tracker with an aperture equal to the size of a single SSD was built with 6 *x,y* planes and interchangeable lead converter foils. The SSDs were instrumented with an early prototype of the front-end readout chip,[5] with minimal digital circuitry. One of the SSD planes was a full ladder, for study of noise issues. The main objective of the beam test, in a tagged-photon beam at the Stanford Linear Accelerator Center (SLAC), was to verify the Monte Carlo simulation being used in designing the LAT. The instrument and the beam-test results are described in detail in.[6] Figure 9 shows the angular resolution measured as a function of gamma-ray energy, for conversions in 4% radiation-length thick converter foils, with the simulations results over plotted for comparison.

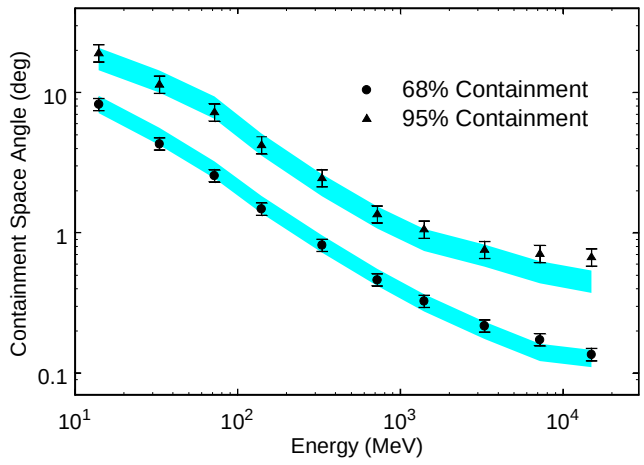

Figure 9. The angular resolution from gamma-ray conversions in the 1997 beam test tracker, compared with Monte Carlo simulations (the solid bands).

7.2 Beam Test Engineering Model (BTEM)

In 1999 we completed a prototype of a full tracker module, although it was built to an earlier design that differs in a number of details from the final design. It was somewhat smaller, with 32 cm long SSD ladders (using SSDs made from 4-inch and 6-inch wafers) and

only 16 *x*,*y* planes, for a total of 51,200 electronics channels. The electronics readout and control scheme followed the description in Figure 6, although many detailed changed have since been made in the final design. The integration of the electronics was similar to the final design, although some improvements have since been made to facilitate manufacturing and quality control. The mechanical structure was made from aluminum, except that carbon-composite face sheets were used on the tray panels. One fully instrumented tray is shown in Figure 10. The BTEM tracker module is described in more detail in Ref. 7.

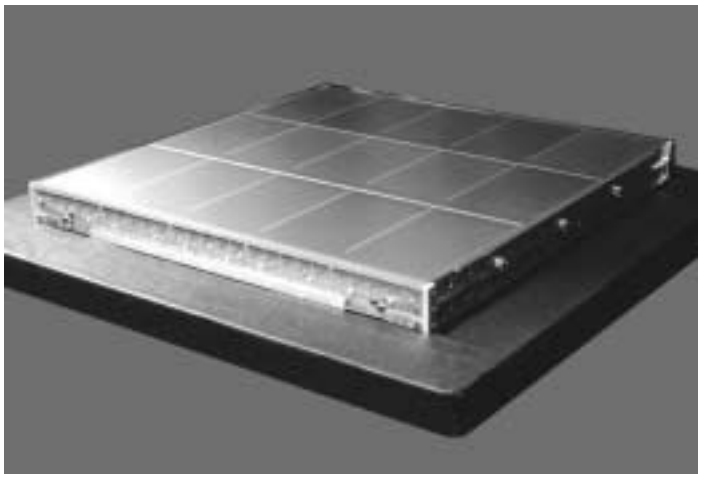

Figure 10. One of 17 trays from the BTEM tracker.

The BTEM tracker module demonstrated excellent performance of the silicon-strip detector system. It consumed 210 microwatts of power per channel, and the detectors achieved essentially >99% efficiency for muons and electrons with noise occupancy equal to a few times 10^{-6}. Figure 11 shows the measurements of efficiency versus threshold for two of the layers, made using beam electrons. The first three points are at greater than 99% efficiency. The noise occupancy for the third point (170 mV threshold) was much less than 10^{-5} for all layers. More information and results from the BTEM can be found in References 7, 8, and 9.

7.3 Balloon Flight

Subsequent to the beam test, the BTEM was refurbished and adapted as a balloon-flight payload. In the summer of 2001 it flew from Palestine, Texas for several hours at an altitude of 38 km. The instrument was triggered by the tracker itself, with the trigger rate rising from a few Hz at ground level to a maximum of about 1200 Hz at the cosmic-ray shower maximum, then falling to about 500 Hz at the float altitude, a rate that agreed with Monte-Carlo simulations based on known cosmic-ray fluxes.

The tracker performed well throughout the flight, with 4.5 million triggers recorded. The temperature was stable, even in the low pressure at altitude (2 psi in the chamber holding the instrument), and there was no problem from the large shocks suffered during parachute opening and landing (up to 50 g acceleration measured by onboard accelerometers). The tracker continued to function normally afterwards, and there was no damage visible inside or out after removing the tracker sidewalls. Publications of measurements made during the flight are in preparation.

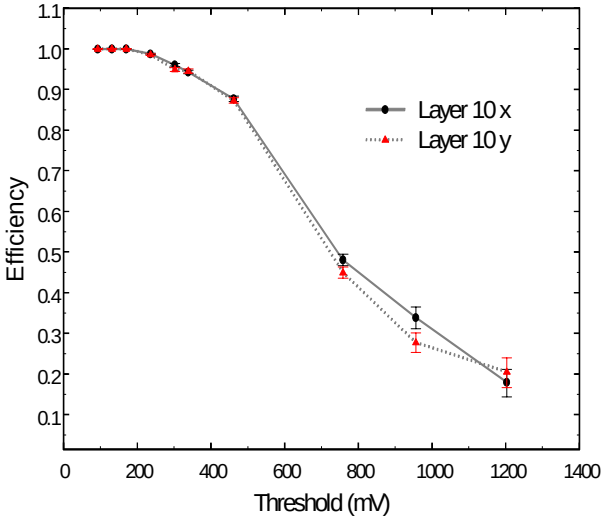

Figure 11. The efficiency for detection of a single test-beam electron versus discriminator threshold, measured in two layers of the BTEM tracker.

7.4 Carbon-fiber prototype mechanical assembly

During the past year we built a mechanical prototype of a single tracker module. It was built according to the flight-instrument design and materials, except that aluminum mass models were substituted for 9 of the 19 trays. The carbon-composite trays were fitted with tungsten converter sheets, bias circuits, and ladders of dummy silicon detectors (aluminized silicon). An aluminum fixture substituted for the grid, and actual flexures and a thermal gasket interfaced it to the module. The purpose was to develop the fabrication techniques for the carbon-

Figure 12. A prototype carbon-composite tray panel.

composite panels, test assembly techniques for the module, carry out mechanical and thermal testing on the panel structures and the module as a whole, and test our models for the dynamical response of the module. This exercise has allowed us to adjust details of the tracker design and the assembly fixtures to resolve problems before proceeding to the critical design review (CDR). Figure 12 shows one of the carbon-composite panels before installation of converters, bias circuits, and silicon.

Individual trays were tested by thermal cycling, vacuum cycling, and vibration. The tray-panel fundamental frequency agreed with FEM predictions and, with tungsten and silicon added, was above the 500 Hz specification (which was derived to ensure that *x*,*y* planes of silicon never hit each other during launch). No damage occurred during random-vibration to levels recommended by GEVS.[10] No damage occurred to the panels or the silicon ladders when thermal cycling 10 times between –30°C and +50°C. The maximum stress in the silicon inferred from strain measurements was about 2000 psi, compared with a mean failure stress of 30,000 psi (σ=6000 psi) that we determined from bend tests of actual detectors. No problems occurred in vacuum cycling—the trays vent well. The flexures worked well in protecting the bottom tray from thermal stress when connected to an aluminum base during thermal cycling.

The entire module was also subjected to random-vibration testing to 12.3 g rms (6 dB beyond the levels expected during launch) along 3 axes with *no* notching at the resonances. Sine-sweeps done before and after the random vibration were used to analyze the resonance modes. The lowest frequencies, about 200 Hz along the vertical axis and just below 100 Hz for lateral motion, correspond to rigid-body motion of the module on its flexure supports. These modes are strongly influenced by the properties of the thermal-gasket compressed between the module and the grid. No damage occurred during vibration along the vertical axis. However, the thermal-gasket between the bottom tray and the aluminum fixture did not recover from compression as well as desired, resulting in a substantial decrease in the module fundamental frequency during the random vibration. Internal motion of the trays was as expected and caused no damage. Vibration on the horizontal axes resulted at full power in failure of some of the inserts in the bottom tray into which the corner flexures mount. To resolve these problems, we are improving the insert design and searching for other gasket materials, perhaps sacrificing some thermal performance for better mechanical properties.

8. STATUS AND CONCLUSIONS

The LAT tracker passed its preliminary design review in January of this year. The CDR is scheduled for January of 2003, but long-lead-time procurements are already in progress, for the SSDs and the carbon-carbon material, and assembly of the SSD ladders will begin this summer. A full “engineering-model” tracker module is being fabricated to the final design and with the final tooling intended for the flight modules. It will be “instrumented” with dummy SSDs and with MCMs loaded with dummy ICs, but including resistors that dissipate the correct amount of heat. This module will be put through the full suite of environmental testing to validate the mechanical and thermal design prior to CDR.

Four additional trays will be fabricated and loaded with fully functional SSDs and readout electronics, to be used for validation of the electronics design prior to CDR.

The first of the 18 tracker modules will be completed about a year following CDR, with the remaining fabricated in the ensuing 6 months. The MCMs will be assembled in the U.S. by Teledyne Electronics Technologies, tested and burned in, and then shipped to Italy for integration onto trays. Ladder and tray assembly will be done at G&A Engineering and at MIPOT in Italy. Plyform, in Italy, will fabricate the tray panels. INFN institutes in Italy will do environmental testing of the trays, assembly of the tracker modules, and testing of the modules before shipping them to SLAC for integration into the LAT.

The LAT, with at least a 30-fold improvement in sensitivity over the previous generation high-energy gamma-ray telescope, promises to make large strides in advancing our knowledge and understanding of the astrophysics of high-energy, nonthermal processes occurring around some of the most exotic objects in the universe. This large improvement in sensitivity is achieved by application of modern detector technology, much of it developed in the field of elementary particle physics. However, to implement such a large million-channel detector in a space mission requires not only advanced technology but also a robust design that can be manufactured with good quality control, can survive intact the launch and orbital environment, and can operate reliably for at least 5 years. The LAT tracker design emphasizes modularity and repetition, redundancy, well-developed and proven technologies (single-sided SSDs, CMOS ICs, polyimide and Kapton circuits, honeycomb composite panels, etc.), and assemblies that are amenable to rapid fabrication by industrial vendors. The design concepts have already been well proven by a series of prototypes, good progress is being made on production tooling and procedures, and we are looking forward to a launch in 2006, followed by many bountiful years of data.

ACKNOWLEDGMENTS

The author's work on the LAT project is supported by DOE grant DE-FG03-92ER40689. The LAT tracker is being designed and built by a collaboration of institutes in Japan, Italy, and the United States, with funding support from NASA, DOE., Mombusho and STA in Japan, and INFN and ASI in Italy.

REFERENCES

1. D.J. Thompson, et al., *ApJS* **86**, p. 629, 1993.
2. R.C. Hartman, et al., *ApJS* **123**, p. 79, 1999.
3. J.V. Osborn, et al., "Single-Event Latchup Characteristics of Three Commercial CMOS Processes," *7th NASA Symposium on VLSI Design*, 1998.
4. L.R. Rockett, Jr., *IEEE Trans. Nucl. Sci.* **35**, No. 6, p. 1682, 1988.
5. R.P. Johnson, *IEEE Trans. Nucl. Sci*. **45**, p. 927, 1998.
6. W.B. Atwood, et al., *Nucl. Instr. Meth.* **A446**, p. 444, 2000.
7. E. Atwood, et al., *Nucl. Instr. Meth.* **A457**, p. 126, 2001.
8. P. Allport, et al., *Nucl. Instr. Meth.* **A466**, p. 376, 2001.
9. E. do Couto e Silva, et al., *Nucl. Instr. Meth.* **A474**, p. 19, 2001.
10. GEVS-SE Rev A, "General Environmental Verification Specification for STS & ELV Payloads, Subsystems, and Components," http://arioch.gsfc.nasa.gov/302/gevs-se/toc.htm.